Biophysical Journal Volume 68 March 1995 1120–1127

Computation of the Electrophoretic Mobility of Proteins

Kyung Sun Chae and Abraham M. Lenhoff
Center for Molecular and Engineering Thermodynamics, Department of Chemical Engineering, University of Delaware,
Newark, Delaware 19716 USA

ABSTRACT A scheme is presented for computing the electrophoretic mobility of proteins in free solution, accounting for the details of the protein shape and charge distribution. The method of Teubner is implemented using a boundary integral formulation within which the velocity distribution, the equilibrium electrical potential around the molecule, and the potential distribution due to the applied field are solved for numerically using the boundary element method. Good agreement of the numerical result is obtained for spheres with the corresponding semi-analytical specialization of Henry's analysis. For protein systems, the method is applied to lysozyme and ribonuclease A. In both cases, the predicted mobility tensors are fairly isotropic, with the resulting scalar mobilities being significantly smaller than for spheres of equal volume and net charge. Comparisons with previously published experimental results for ribonuclease show agreement to be excellent in the presence of a net charge, but poorer at the point of zero charge. The approach may be useful for evaluating approximate methods for estimating protein electrophoretic mobilities and for using electrophoretic measurements to obtain insight into charge distributions on proteins.

INTRODUCTION

Despite the widespread use of electrophoresis for the analysis and separation of proteins and other biological materials, the relation of observable electrophoretic behavior to the underlying molecular structure remains incomplete. The electrophoretic mobility is the key parameter characterizing the motion of a charged particle in an electric field in free solution, and although its general dependence on the size and net charge of the particle is well known, a detailed relationship is still lacking for molecules with the complexity of shape and charge distribution of relatively rigid proteins. Even greater complexity arises when conformational changes are considered or when the stochastic configurational aspects that arise with polyelectrolytes such as nucleic acids are considered. Ultimately, all of these features may also interact with a structured medium such as occurs in polyacrylamide gel electrophoresis.

In this paper, we consider the first of these levels of analysis, namely, the relation of the electrophoretic mobility of a rigid protein in free solution to the molecular structure. The protein electrophoretic mobility is influenced by the protein amino acid composition, size, and shape and by the solution ionic strength, pH, viscosity, and temperature. These parameters generally are reduced to a measure of the protein size and the net charge Q, and the electrophoretic mobility is then calculated using classical electrophoresis theory, derived for spheres. In this approximation, macromolecules are treated as nonconducting spheres with a uniform surface charge or potential, and the electrophoretic mobility represents a balance between the electrostatic force driving the particle and the hydrodynamic drag retarding it. The latter includes a contribution due to flow of mobile ions in the double layer, the electrophoretic retardation force, and because the charge density involved is strongly dependent on the ionic strength, this parameter affects the particle mobility. The dependence is captured by a simple analysis yielding exact results in two well known limiting situations, namely, where the Debye thickness is either infinitely large or infinitely small (see, e.g., Mosher et al., 1992).

For thick double layers, the electrophoretic velocity, U, of a rigid particle of radius a in an applied electric field of strength E is (Mosher et al., 1992)

$$\frac{U}{E}=\frac{2\epsilon\psi_0}{3\eta} \tag{1}$$

which is the Debye-Hückel approximation (Debye and Hückel, 1924; Hückel, 1924). Here ψ_0 is the uniform surface potential of the particle and ϵ and η are the dielectric permittivity and the viscosity of the fluid, respectively. For very thin double layers, the limiting approximation is from the Helmholtz-Smoluchowski theory (von Smoluchowski, 1921) and yields

$$\frac{U}{E}=\frac{\epsilon\psi_0}{\eta}. \tag{2}$$

The transition between these two limits is given by Henry's (1931) formula, valid for all values of the double layer thickness:

$$\frac{U}{E}=\frac{\epsilon\psi_0}{\eta}f_1(\kappa a)=\frac{Q}{4\pi\eta a(1+\kappa a)}f_1(\kappa a), \tag{3}$$

where the Henry function f_1, which reflects the dependence on the Debye parameter, κ, increases monotonically from ⅔ to 1.

One additional noteworthy factor in the classical theory of the electrophoresis of spherical particles is the deformation

---

Received for publication 26 September 1994 and in final form 19 December 1994.

Address reprint requests to Dr. Abraham M. Lenhoff, Center for Molecular and Engineering Thermodynamics, Department of Chemical Engineering, University of Delaware, Newark, Delaware 19716. Tel.: 302-831-8989; Fax: 302-831-4466; E-mail: lenhoff@che.udel.edu.

0006-3495/95/03/1120/08 $2.00

of the electric double layer around the particle. The resulting relaxation effect may make a significant contribution when the thickness of the double layer is comparable with the particle radius and when the potentials are high (O'Brien and White, 1978).

These results have been applied in several ways to interpreting and predicting protein electrophoretic mobilities. An implicit assumption that is usually made is that the molecules are spherical, although Norde and Lyklema (1978) treated human serum albumin as a cylinder in view of its relatively large aspect ratio. For the sphere approximation, different approaches have been used to estimate the effective radius. Norde and Lyklema (1978) used a value suggested by the molecular volume plus a surrounding hydration shell, whereas Compton (1991) extended this to account for both hydration and asymmetry as estimated using the frictional ratio. Mosher et al. (1989), on the other hand, estimated the radius from the experimental translational diffusivity.

The net charge in some cases has been estimated based on the protein amino acid composition and the intrinsic pK_a values of the different residues (Mosher et al., 1989; Compton, 1991). Both of these studies noted the known discrepancy at some pH values between this method of estimating net charge and actual protein titration experiments. A different approach was taken by Norde and Lyklema (1978), who used their experimental data to estimate the zeta potential of ribonuclease A as a function of pH and ionic strength.

In all of these studies, two major approximations were made, namely, that the molecules are spherical and that the net charge or the mean surface potential adequately characterizes the charge distribution. The hydrodynamic aspects are obviously affected by the first approximation, whereas the electrostatic and the electrophoretic retardation forces are affected by both approximations. Several treatments are available in which these assumptions have been relaxed; cases studied include spheres with nonuniform surface potential (Anderson, 1985; Solomentsev et al., 1993) or internal charge (Yoon, 1991) distributions and ellipsoids with uniform (Yoon and Kim, 1989) and nonuniform (Fair and Anderson, 1989) surface potential distributions.

Other studies have dealt more specifically with proteins. The effect of shape on electrostatics was investigated by Haggerty and Lenhoff (1991), who used detailed molecular electrostatics computations, accounting for both molecular shape and charge distribution, to calculate the mean surface potential of ribonuclease A as a function of pH for comparison with the zeta potential estimates of Norde and Lyklema (1978). The effect of protein shape on purely hydrodynamic behavior, on the other hand, was studied by Brune and Kim (1993), who calculated rotational and translational diffusivities of lysozyme using the crystal structure and found excellent agreement with experimental values.

Despite all of these previous efforts, none has accounted explicitly for the effect of the details of protein shape and charge distribution on both electrostatics and hydrodynamics; consequently, it has not yet been possible to attribute discrepancies between theory and experiment definitively to any particular approximation. In this work, we seek to address this shortcoming by evaluating the electrophoretic mobility tensors of proteins by an application of Teubner's (1982) approach. This method is based on the observation that the electrical potential can be decoupled from the flow field and considered separately. We compute both fields using the boundary element method (BEM) and combine the information obtained from both by numerical quadrature.

The rest of the paper is organized as follows. We first present the integral equations for the electrostatic potentials and hydrodynamics of macromolecules of arbitrary shape and internal charge distribution. Next the numerical implementation of the BEM is described. As an initial test of the method, the mobility tensor of a spherical particle in a uniform dielectric medium was calculated using the BEM, and compared with the semi-analytic calculation. We then turn our attention to the main focus of the paper, the electrophoretic mobility tensor of proteins. Lysozyme and ribonuclease A are used as model proteins because they are single-domain globular proteins with known three-dimensional structures.

METHODS

Electrophoretic motion

The analysis of electrophoresis is essentially a study of the balance between the applied electrical force and the hydrodynamic drag. In our analysis, we follow the general scheme developed by Teubner (1982), who used the linearity of the Stokes equation and the reciprocal theorem of Lorentz in evaluating the forces. The hydrodynamic force on a charged particle was decomposed into the force with all electric effects suppressed plus an excess term, the electrophoretic retardation force, depending only on the electric field. Two assumptions were made in simplifying the equations to estimate mobility tensors. First, the applied field was considered small compared with the field because of the equilibrium double layer. Neglecting the deformation of the double layer due to the applied field, the potentials around the particle were decomposed into two independent contributions: ψ from the equilibrium double layer and ϕ_j from the j component of the ambient field. Second, the coupling tensors (linking translational and rotational motion) were neglected. The electrophoretic mobility was then simply obtained by equating the total force to zero, yielding the final result:

$$U = (1/\eta)K^{-1}GE^0 \tag{4}$$

for the translational electrophoretic motion of a charged particle in an electric field. Here K and E^0 are the translation tensor of an uncharged particle and the spatially uniform external field, respectively, and the tensors G and K are given by

$$G_{ij} = \epsilon \int_G (\bar{V}^i_k - \delta_{ik})\left(\Delta\psi + \frac{\partial\phi_j}{\partial x_k}\right) d^3r \tag{5}$$

$$K_{ij} = -\int_S \bar{\sigma}^i_{jl} n_l \, dS. \tag{6}$$

Here $\bar{V}^i_k$ represents the k component of the Stokes flow field caused by a translating sphere with a unit velocity along the i axis and $\bar{\sigma}^i$ corresponding stress tensor, and the integrals are over the exterior volume and the surface, respectively.

Analytical solutions of these equations exist for some simple geometries, but more complicated cases can be treated only by approximate numerical methods. For the spherical particle, Yoon and Kim (1989) derived the electrophoretic mobility using Teubner's method and the linearized Poisson-Boltzmann equation as

$$U = \frac{3QE^0}{1 + \kappa a}\left[\frac{1}{2} + \int_a^\infty e^{-\kappa r}\left(\frac{a^4}{r^5} - \frac{5a^6}{2r^7}\right)\mathrm{d}r\right], \tag{7}$$

which is a special case of Henry's (1931) result, to be evaluated semi-analytically.

To determine the electrophoretic mobility of arbitrary particles with finite double layers, a numerical solution is required. A solution under the assumptions of this section requires three boundary-value problems to be solved: the Poisson-Boltzmann equation to obtain ψ, Laplace's equation to obtain ϕ_j, and the Stokes equation for the translation of an uncharged particle through a quiescent fluid to obtain the velocity field $\bar{V}^{i}_{k}$ and the translation tensor K. An integral formulation has been used for each in this work, leading to a BEM solution in each case. These aspects are discussed below.

Integral formulation

Equilibrium potential

The conceptual approach generally used to determine the equilibrium potential distribution around a protein molecule in an electrolyte solution has its origins in the work of Kirkwood (1934), but most of the implementation in a physically realistic fashion has taken place since the early 1980s. The present work follows the solution of Yoon and Lenhoff (1990), where much of the other relevant work is summarized. The protein is represented as a dielectric cavity B^i with an internal distribution of point charges of magnitudes q_k located at positions x_k. The interior potential ψ^i is given by the Poisson equation

$$\nabla^2\psi^i(x) = -\frac{1}{\epsilon^i}\sum_{k=1}^{n} q_k\delta(x - x_k) \qquad \text{for} \quad x \in B^i. \tag{8}$$

The exterior potential ψ^e in the domain B^i is assumed to be governed by the linearized Poisson-Boltzmann equation

$$\nabla^2\psi^e(x) = \kappa^2\psi^e(x) \qquad \text{for} \quad x \in B^e. \tag{9}$$

These equations are solved subject to a zero potential condition far from the molecule, and continuity of the potential and the normal component of the electric displacement at the bounding surface. The integral formulation and the approach to solving it are given elsewhere (Yoon and Lenhoff, 1990).

Ambient potential

In regions of uniform dielectric constant that have no free charges, the electrostatic potential ϕ_j must satisfy Laplace's equation,

$$\nabla^2\phi_j(x) = 0. \tag{10}$$

At the surface of an insulating particle of zero dielectric constant, the electric field normal to the surface vanishes, and although a protein molecule has a finite dielectric constant, it is small enough relative to that of the surrounding aqueous medium for the discrepancy in neglecting in the internal field to be negligible. Far from the particle, the potential approaches the uniform applied electric field. These boundary conditions are expressed as

$$\phi_j|_{r\to\infty} = -E_j x_j \qquad \text{and} \qquad \left.\frac{\partial\phi_j}{\partial n}\right|_{\partial B} = 0. \tag{11}$$

From the boundary condition at infinity we can take the ambient potential to be of the form

$$\phi_j(x) = \phi_j^\infty(x) + \phi_j^1(x), \tag{12}$$

where the first term represents the potential due to the applied field in the absence of the particle and the second term represents the perturbation due to the particle. Substituting this expression in Eq. 11 gives the boundary condition on the perturbation potential:

$$\phi_j^1|_{r\to\infty} = 0 \qquad \text{and} \qquad \left.\frac{\partial\phi_j^1}{\partial n}\right|_{\partial B} = n_j E_j. \tag{13}$$

The boundary integral equation for the ambient potential then becomes

$$\begin{aligned}\phi_j(x) = \phi_j^\infty(x) &+ \frac{1}{4\pi}\int_{\partial B}\phi_j^1\frac{\partial}{\partial n}\left(\frac{1}{|x - x'|}\right)\mathrm{d}A(x') \\ &- \frac{1}{4\pi}\int_{\partial B}\frac{\partial\phi_j^1}{\partial n}\frac{1}{|x - x'|}\mathrm{d}A(x') \qquad \text{for} \quad x \in B^e\end{aligned} \tag{14}$$

in the external domain and

$$\begin{aligned}\phi_j^{1s}(x^s) = &\frac{1}{2\pi}\int_{\partial B}\phi_j^{1s}\frac{\partial}{\partial n}\left(\frac{1}{|x^s - x'|}\right)\mathrm{d}A(x') \\ &- \frac{1}{2\pi}\int_{\partial B}\frac{\partial\phi_j^{1s}}{\partial n}\frac{1}{|x^s - x'|}\mathrm{d}A(x')\end{aligned} \tag{15}$$

on the boundary. The integral equation (15) is solved for the surface ambient potential when surface tractions are specified. Finally, to obtain the potential gradient throughout the external domain for use in Eq. 5, Eq. 14 is differentiated with respect to the source point to give

$$\begin{aligned}\nabla\phi_j(x) = \nabla\phi_j^\infty(x) &+ \frac{1}{4\pi}\int_{\partial B}\phi_j^1\nabla\frac{\partial}{\partial n}\left(\frac{1}{|x - x'|}\right)\mathrm{d}A(x') \\ &- \frac{1}{4\pi}\int_{\partial B}\frac{\partial\phi_j^1}{\partial n}\nabla\left(\frac{1}{|x - x'|}\right)\mathrm{d}A(x').\end{aligned} \tag{16}$$

Hydrodynamic velocity

The Stokes flow past an arbitrary particle is described by

$$\nabla\cdot v^i(x) = 0, \qquad -\nabla p^i(x) + \eta\nabla^2 v^i(x) = 0 \qquad \text{for} \quad x \in B^e \tag{17}$$

$$v^i|_{\partial B} = U^i \qquad \text{and} \qquad v^i|_{r\to\infty}, p^i|_{r\to\infty} = 0, \tag{18}$$

where v is the velocity vector and p is the pressure. We use a Fredholm integral equation of the first kind to solve this problem. This formulation is straightforward because it directly involves physical variables such as the velocities and the tractions on the boundaries. Although it is well known that the formulation of the first kind is ill-posed, this drawback does not appear in certain situations (Youngren and Acrivos, 1975; Hsiao, 1987; Chan et al., 1992), including the present problem. For flow in an unbounded domain the integral representation is given by

$$\begin{aligned}v^i(x) = &\frac{1}{8\pi}\int_{\partial B} f^i\left(\frac{\delta_{km}}{r} + \frac{r_k r_m}{r^3}\right) dA(x') \\ &+ \frac{1}{8\pi}\int_{\partial B} v^i\left(\frac{6r_k r_m}{r^5}\right)(n\cdot r)\,\mathrm{d}A(x'),\end{aligned} \tag{19}$$

where and $r = |x - x'|$ and f^i is the local surface stress. If U^i is constant, the no-slip boundary condition leads to the following linear integral equations:

$$U^i = \frac{1}{8\pi}\int_{\partial B} f^i\left(\frac{\delta_{km}}{r} + \frac{r_k r_m}{r^3}\right)\mathrm{d}A(x') \qquad \text{for} \quad x \in \partial B. \tag{20}$$

Thus, when the Stokes problem is formulated in this manner, f^i is determined directly and the total force F^i acting on the particle is obtained from

$$F^i = \int_{\partial B} f^i\,\mathrm{d}A(x'). \tag{21}$$

In the absence of rotational motion, Eq. 21 may be written in the form

$$F^i = -\eta K_{ij} U_j, \tag{22}$$

where the translation tensor, K_{ij}, is a purely geometric property of the particle. It is dependent on its size and shape but independent of the orientation and the fluid properties (Happel and Brenner, 1983). It is from this equation that we find the translation tensor for use in Eq. 4.

Numerical procedures

To implement the BEM for a protein, the molecular boundary as defined by the crystal structure was discretized into a set of flat linear triangular elements using the Molecular Surface Program of Connolly (1993). Very short edges were removed by combining the two defining nodes at the midpoint. Charges were placed at the locations of the ionizable side chains, with their magnitudes depending on the solution pH as calculated using the Henderson-Hasselbalch equation. In all BEM calculations, the values of the unknowns on each element were written in terms of their values at nodal points by assuming linear dependence over the element.

Although the BEM has the advantage of reducing the dimensionality of the problem, the method is demanding in that the numerical integration required for calculation of the boundary integrals must be performed accurately and efficiently to optimize the accuracy and computation time of the whole analysis. We have investigated the effects on performance of the number of quadrature points. To evaluate potentials at the surface when the maximum degree of singularity is -2, a six-point Gaussian quadrature formula was used on each element, except for $x_j\, dA_j$, where three- or one-point Gaussian quadrature formulae reduced the effect of the singularity. A six-point quadrature rule, however, was used for all elements in solving the hydrodynamic problem because the degree of singularity is just -1.

Once the surface values of the dependent variables (velocities and potentials) are known, their values at any points in the domain can be found directly by quadrature using Eqs. 16, 19, and the corresponding equation for the equilibrium potential (Eq. 5 in Yoon and Lenhoff, 1990). The main objective in seeking these results is to evaluate the integrals for the mobility tensors in Eqs. 5 and 6. The functions ψ and $\bar{V}_k^i$ in the domain are readily computed, but the gradient of ambient potential defined by Eq. 16 and used in Eq. 5 is more problematic. Nearly hypersingular behavior occurs whenever the source point is close to the surface on which the integrations have to be performed. Nearly singular integrals must be transformed into nonsingular integrals or at worst weakly singular integrals before applying any numerical quadrature. Several advanced techniques to handle hypersingularities have been developed recently (Krishnasamy et al., 1990; Guiggiani et al., 1992; Guiggiani, 1993; Liu et al., 1993; Rudolphi and Youn, 1993; Sladek et al., 1993); of these, the kernel cancellation method (Liu et al., 1993) was used. The method, based simply on subtracting two integral equations, evaluated at the point close to the surface and its image point, shows considerable improvement in accuracy for the interior field evaluations at points close to the boundary. When the source point is close to the surface, we apply this method in Eq. 16 and obtain the alternative integral representation

$$\nabla\phi_j(x) = \nabla\phi_j^{\infty}(x) - \frac{1}{2\pi}\int_{\partial B} \frac{\partial\phi_j^1}{\partial n}\nabla\left(\frac{1}{|x - x'|}\right) dA(x'), \tag{23}$$

which is much more effective for calculations close to the boundary.

The volume integral in Eq. 5 was evaluated using the NAG routine D01GBF (Numerical Algorithms Group, Downers Grove, IL), which is based on an adaptive Monte Carlo method. The electrophoretic mobility tensor for an arbitrary particle was then found from Eq. 4.

RESULTS

The numerical algorithms implemented to solve the equations discussed above were tested for accuracy by comparing them to Henry's (1931) semi-analytic result (Eq. 7) for a sphere. Using parameters suggested by hen egg lysozyme at pH 7, a sphere of radius 15 Å with a point charge of +8 at the center was examined. Other parameter values were: interior dielectric constant $\epsilon^i = 4$; homogeneous, isotropic medium of $\epsilon^e = 78$ and $\eta = 8.95 \times 10^{-4}$ Pa s at 25°C; Debye length $\kappa^{-1} = 9.61$ Å, corresponding to 0.1 M of a 1:1 electrolyte. Table 1 shows the electrophoretic mobility of the spherical particle as calculated using our numerical algorithms for four different surface tesselations. Although the accuracy does not improve monotonically with mesh refinement, the mobility values computed using the BEM are in good agreement with the corresponding analytical results, and the numerical calculations thus can be applied to electrophoretic mobility computations for real protein models.

For applications to proteins, we computed the electrophoretic mobility for hen egg lysozyme and bovine pancreatic ribonuclease A. Some of the parameters relevant to these calculations are summarized in Table 2. Cases examined include both the full electrophoretic mobility calculations as well as corresponding studies using the semi-analytic calculation based on the sphere idealization. For the sphere cases, the effective radii of the proteins were calculated from the molecular weights assuming spherical molecules with a specific volume of 0.74 cm^3/g. The frictional ratio, which corrects for protein asymmetry and hydration (Creighton, 1993), usually varies from about 1.0 to 1.4 for globular proteins. The effective radius for both proteins becomes 16 Å when this ratio is 1.0 and 20 Å when it is 1.25. The calculations of the full mobility tensors were performed for pH 7 and ionic strengths of 0.1 M for lysozyme and 0.05 M for ribonuclease. The structures used were taken from the Brookhaven Protein Data Bank (Bernstein et al., 1977). All acidic residues and the COOH terminus were assumed to be deprotonated, and all basic residues and the NH$_2$ terminus were assumed to be protonated, apart from His residues, which were taken to be neutral. The tesselations used for the proteins were both significantly finer than for the spheres shown in Table 1; this is appropriate given the proximity of numerous charges to the protein surface (Yoon and Lenhoff, 1990). Using the semi-analytical result for the sphere as reference, the appropriate domain size for quadrature in Eq. 5 was estimated as a 200-Å cube.

Table 3 gives the computed mobility tensors of lysozyme and ribonuclease. In both cases, the tensors show an isotropic tendency. Moreover, because the off-diagonal elements are small, calculation of just the diagonal elements of G provides computational economy with little loss of accuracy.

TABLE 1 Numerical results for sphere

Number of surface triangles	Number of nodal points	Electrophoretic mobility ($\times 10^{-4}$ cm^2/V s)	Error* (%)
240	122	1.972	2.47
720	362	1.988	1.68
960	482	2.025	0.15
1280	642	1.987	1.73

*$U_{\text{anal}} = 2.022 \times 10^{-4}$ cm^2/V s from Eq. 7.

TABLE 2 Physical and numerical parameters of the model proteins

Protein	Molecular weight	Surface area (Å^2)	Equivalent radius* (Å)	Dielectric constant	Number of surface triangles	Number of nodal points
Lysozyme	14300	5010	16.1	4	3690	1847
Ribonuclease	13700	5175	15.9	4	4884	2444

*For sphere of equal volume.

TABLE 3 Computed mobility tensors

Lysozyme (pH 7, 0.1 M) ($\times 10^{-4}$ cm^2/V s)			Ribonuclease (pH 7, 0.05 M) ($\times 10^{-4}$ cm^2/V s)		
1.4856	−0.0335	0.0759	0.6131	−0.0218	−0.0614
−0.0379	1.154	−0.0435	−0.0039	0.6094	−0.0016
0.1377	−0.0271	1.4463	−0.0512	0.0009	0.5715

The physical significance of the computations must be assessed by comparison with experimental data. In general, experimental electrophoretic mobility data are average values in view of the dominance of the orientational distribution by Brownian motion; because the rotational Péclet numbers (Anderson, 1985) are small for the surface potential dipole moments seen in this work, the mean electrophoretic mobility can be represented by (Stigter, 1978; Teubner, 1982):

$$U = \frac{1}{3\eta}\,\mathrm{Tr}(K^{-1}G)E^{0}, \qquad (24)$$

where Tr denotes the trace of the tensor. Applying this to the tensors in Table 3 shows the scalar mobility of lysozyme to be about double that of ribonuclease. The different electrophoretic mobilities can arise mainly from either differences in net charge and charge distribution or a difference in size. Because the net charges determined for lysozyme and ribonuclease at neutral pH are +8 and +4, respectively, and the proteins' molecular weights are almost equal, the observed difference is attributable primarily to the net charge.

We examine the predicted scalar mobilities more extensively by varying the ionic strength of the electrolyte. In Fig. 1, the plot of mean mobility versus buffer concentration shows a decrease in mobility with increasing ionic strength for both the full molecular description of lysozyme and for the corresponding values for spheres. For the sphere result (Eq. 7), effective radii of 16 and 20 Å were used; the former yields a sphere of volume approximately equal to the true molecular volume, whereas the latter leads to a much better estimate of the electrophoretic mobility. Because of the screening effect of the electrolyte, the surface potential should decrease with increasing ionic strength, and this explains most of the trend observed. As regards the effectiveness of the sphere model, a good correlation is seen between the full calculations and the 20-Å sphere results at moderate ionic strength, but at high ionic strength the discrepancy is much larger.

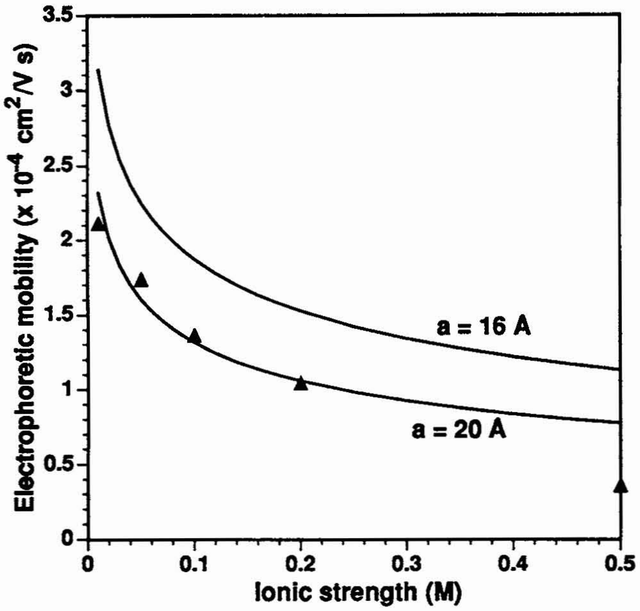

FIGURE 1 Comparison of electrophoretic mobility of lysozyme at pH 7 as a function of ionic strength calculated using the full molecular description (*points*) and the semi-analytical result for spheres (Eq. 7); sphere results are shown for two values of molecular radius (*lines*).

The effects of net charge and charge distribution, key parameters intrinsic to the protein that affect the electrophoretic mobility, were investigated for ribonuclease A by comparing calculated and measured (Norde and Lyklema, 1978) mobilities at pH 7 and at the point of zero charge (pzc), for 0.05 M 1:1 electrolyte. The charge distribution around the pzc of ribonuclease must be specified with some care, mainly because not all of the Tyr residues are titratable, as first found by Shugar (1952) and Tanford et al. (1955). The latter work suggested that three of the six Tyr residues titrate in the normal pH range, but subsequent studies questioned this result. The controversy was resolved by NMR experiments that determined that four of the residues are titratable (Egan et al., 1978; Lenstra et al., 1979; Tanokura, 1983), with the last of these providing pK_a values for the titratable residues (around pH 10). Lys residues, of which there are 10 in ribonuclease, also titrate around pH 10, but pK_a values for individual residues are not available; Tanford and Hauenstein (1956) suggest an effective pK_a of 10.2 for these residues, but a range of values is possible for Lys residues in general (Nozaki and Tanford, 1967). Using a pK_a of 10.2 for all Lys residues, the pzc is calculated to be 9.59, which is in good agreement

TABLE 4 Scalar electrophoretic mobilities of ribonuclease A (0.05 M)

	Surface potential (mV)		Mean mobility ($\times 10^{-4}$ cm^2/V s)	
pH	Computed (this work)	Measured*	Computed (this work)	Measured*
7	19.8	9.8	0.598	0.55
9.59	−3.2	−4.6	0.035	−0.24

*Norde and Lyklema (1978). Surface potentials evaluated using Henry's (1931) result. pH 9.59 values obtained by interpolation.

with experiment (Tanford and Hauenstein, 1956; Norde and Lyklema, 1978; Bergers et al., 1993).

The electrophoretic mobility results are summarized in Table 4, with positive values obtained at both pH values. This is expected for pH 7 in view of the net charge of +4, and the calculated mean surface potential is also consistent. At the pzc, however, the computed mobility is slightly positive but, interestingly, the computed mean surface potential at this point is negative.

DISCUSSION

Assessing the value of the approach developed here requires comparison of the computed electrophoretic mobilities of proteins with experimental data; we do so for both ribonuclease A and lysozyme. The ribonuclease data are those of Norde and Lyklema (1978), who reported the electrophoretic mobility in free solution of ribonuclease A at a number of pH values and ionic strengths of 0.01 and 0.05 M. We use only the latter results because linearization of the Poisson-Boltzmann equation is more questionable at 0.01 M. At pH 7 excellent agreement between computed and experimental results is seen, whereas use of Henry's result would require increasing the radius to about 20 Å to reduce the predicted mobility to the experimental value. As a result, the effective zeta potential extracted from their data by Norde and Lyklema (1978) is lower than our computed value by about a factor of two. At the pzc, however, our computed mobility is slightly positive, whereas the experimental value is slightly negative. Although we have explored the effects of changing the charge distribution, mainly by changing the Lys pK_a, the computed mobilities remain positive. Possible explanations include the existence of a distribution of pK_a values for the 10 Lys residues, effects of nonlinearities, deviations from the protein crystal structure, or possible other, unaccounted for subtleties in modeling the electrical double layer.

The lysozyme results are comparable with the high performance capillary electrophoresis data of Swedberg (1990), obtained for 0.25 and 0.5 M ammonium phosphate buffer at neutral pH. Unfortunately, however, because of uncertainties regarding temperature, electroosmotic flow, and protein adsorption as well as the complex nature of the electrolyte, a detailed comparison is not meaningful, and we have been unable to find an alternative, more appropriate data set.

The ratio of lysozyme to ribonuclease mobility at pH 7 and 0.05 M ionic strength is somewhat higher than the 2:1 ratio suggested by the net charge, indicating that charge distribution may be a significant factor. Note that although ribonuclease has a relatively large dipole moment (Barlow and Thornton, 1986), its electrophoretic mobility tensor is nearly isotropic with very small off-diagonal elements. This is consistent with the results of Anderson (1985) and Yoon (1991), who showed the dipole moment to have no effect on the translational electrophoretic mobility tensor of a Brownian sphere. The sharp drop in the mobility of lysozyme predicted at 0.5 M ionic strength (Fig. 1) may be another indication of the role of the charge distribution combined with molecular shape: as the Debye length becomes smaller, much of the double layer lies in clefts on the protein surface.

The comparison between calculated electrophoretic mobilities and experimental results is satisfactory given that no adjustable parameters are involved in the calculations. In contrast, if the sphere model is used for the two proteins examined here, it is necessary to use effective sphere radii much larger than suggested by the protein volume (~20 vs. 16 Å) to provide a satisfactory match with experiment at moderate ionic strengths (see Fig. 1). The origins of this behavior can be decomposed into hydrodynamic and electrostatic components. Appropriate hydrodynamic resistances can be attained with radii of about 18 Å, but even a radius increase of this magnitude does not reduce the surface potential of an equivalent sphere far enough for the electrophoretic mobility (Eq. 3) to agree with experiment. Our results suggest that the past use of relatively large effective radii with the Henry model (e.g., Norde and Lyklema, 1978; Compton, 1991) are appropriate, but not for the reasons usually given (e.g., hydration).

There are four potential sources of error in our calculations. The first is the assumption of a classical two-dielectric model, but an important motivation of this work is precisely to examine the success of mobility calculations in the absence of more elaborate model features. The second is the neglect of relaxation effects, which the results of O'Brien and White (1978) suggest to be unimportant for parameter values of interest for protein electrophoresis. The third lies in the various numerical solutions used. The BEM is at its worst in the region very close to the protein surface (Yoon and Lenhoff, 1990), which is a significant fraction of the double-layer region only at high ionic strengths. The domain size has little effect on the electrophoretic mobility as long as it extends well beyond one Debye length from the surface: the disturbances to both the applied electric field and the fluid velocity field caused by the moving particle in an unbounded fluid decay as r^{-3} (Eqs. 17 and 20), whereas the equilibrium field decays exponentially. Overall, the results for the four different surface tesselations (Table 1) indicate that the numerical evaluation is of acceptable accuracy. However, the accuracy can be enhanced by increasing the order of the basis functions for the surface elements.

The final possible source of error, use of the linearized Poisson-Boltzmann equation, rests on the assumption that the potential of a counterion in the solvent region is less than kT. Thus, at 25°C potentials should be less than about 25.7

mV, although the results of O'Brien and White (1978) for spheres suggest that this is a very conservative threshold. The average surface potentials of lysozyme over a range of 0.01–0.5 M in ionic strength and neutral pH indicate that the Debye-Hückel approximation is valid except for the 0.01 M case. As expected, average surface potentials of ribonuclease are smaller than those of lysozyme at the same ionic strengths due to the lower net charge. In either case, however, the low potential condition may not be satisfied in regions where an internal point charge is very close to the molecular surface, but this affects too small a fraction of the domain of interest to warrant a full nonlinear solution.

In summary, we have presented a detailed numerical solution to the equations governing the electrophoresis of proteins, and we have found good agreement with experiment without the need for adjustable parameters, especially adjustments to the effective radius. Although this method is too computationally demanding to be applied to routine electrophoresis measurements, it helps to illustrate both the strengths and weaknesses of the equivalent sphere approach using Henry's (1931) result. It may also be useful in more detailed investigations of charge distributions of proteins.

We thank A. N. Beris and S. Kim for useful discussions.
This work was supported by the National Science Foundation (grant number CTS-9111604).

REFERENCES

Anderson, J. L. 1985. Effect of nonuniform zeta potential on particle movement in electric fields. *J. Colloid Interface Sci.* 105:45–54.

Barlow, D. J., and J. M. Thornton. 1986. The distribution of charged groups in proteins. *Biopolymers.* 25:1717–1733.

Bergers, J. J., M. H. Vingerhoeds, L. van Bloois, J. N. Herron, L. H. M. Janssen, M. J. E. Fischer, and D. J. A. Crommelin. 1993. The role of protein charge in protein-lipid interactions. pH-dependent changes of the electrophoretic mobility of liposomes through adsorption of water-soluble, globular proteins. *Biochemistry.* 32:4641–4649.

Bernstein, F. C., T. F. Koetzle, G. J. B. Williams, E. F. Meyer, M. D. Brice, J. R. Rodgers, O. Kennard, T. Shimanouchi, and M. J. Tasumi. 1977. The Protein Data Bank: a computer-based archival file for macromolecular structures. *J. Mol. Biol.* 112:535–542.

Brune, D., and S. Kim. 1993. Predicting protein diffusion coefficients. *Proc. Natl. Acad. Sci. USA.* 90:3835–3839.

Chan, C. Y., A. N. Beris, and S. G. Advani. 1992. Second-order boundary element calculations of hydrodynamic interactions between particles in close proximity. *Int. J. Num. Meth. Fluids.* 14:1063–1086.

Compton, B. J. 1991. Electrophoretic mobility modeling of proteins in free zone capillary electrophoresis and its application to monoclonal antibody microheterogeneity analysis. *J. Chromatogr.* 559:357–366.

Connolly, M. L. 1993. The molecular surface package. *J. Mol. Graph.* 11:139–141.

Creighton, T. E. 1993. Proteins: Structures and Molecular Properties, 2nd ed. W. H. Freeman and Co., New York. 507 pp.

Debye, P., and E. Hückel. 1924. Bemerkungen zu einem Satze über die kataphoretische Wanderungsgeschwindigkeit suspendierter Teilchen. *Physik. Z.* 25:49–52.

Egan, W., H. Shindo, and J. S. Cohen. 1978. On the tyrosine residues of ribonuclease A. *J. Biol. Chem.* 253:16–17.

Fair, M. C., and J. L. Anderson. 1989. Electrophoresis of nonuniformly charged ellipsoidal particles. *J. Colloid Interface Sci.* 127:388–400.

Guiggiani, M. 1993. Hypersingular integral equations and super-accurate stress evaluation. *In* Boundary Elements XV, Vol. 1. Fluid Flow and Computational Aspects. C. A. Brebbia and J. J. Rencis, editors. Computational Mechanics Publications, Southampton, U.K. 413–428.

Guiggiani, M., G. Krishnasamy, T. J. Rudolphi, and F. J. Rizzo. 1992. A general algorithm for the numerical solution of hypersingular boundary integral equations. *J. Appl. Mech.* 59:604–614.

Haggerty, L., and A. M. Lenhoff. 1991. Relation of protein electrostatics computations to ion-exchange and electrophoretic behavior. *J. Phys. Chem.* 95:1472–1477.

Happel, J., and H. Brenner. 1986. Low Reynolds Number Hydrodynamics. Martinus Nijhoff Publishers, Dordrecht, The Netherlands. 553 pp.

Henry, D. C. 1931. The cataphoresis of suspended particles. I. The equation of cataphoresis. *Proc. R. Soc. A.* 133:106–129.

Hsiao, G. C. 1987. On the stability of boundary element methods for integral equations of the first kind. *In* Boundary Elements IX, Vol. 1. Mathematical and Computational Aspects. C. A. Brebbia, W. L. Wendland, and G. Kuhn, editors. Computational Mechanics Publications, Southampton, U.K. 177–191.

Hückel, E. 1924. Die Kataphorese der Kugel. *Physik. Z.* 25:204–210.

Kim, S., and S. J. Karrila. 1991. Microhydrodynamics: Principles and Selected Applications. Butterworth-Heinemann, Boston, MA. 507 pp.

Kirkwood, J. G. 1934. Theory of solutions of molecules containing widely separated charges with special applications to zwitterions. *J. Chem. Phys.* 2:351–361.

Krishnasamy, G., L. W. Schmerr, T. J. Rudolphi, and F. J. Rizzo. 1990. Hypersingular boundary integral equations: some applications in acoustic and elastic wave scattering. *J. Appl. Mech.* 57:404–414.

Lenstra, J. A., B. G. J. M. Bolscher, S. Stob, J. J. Beintema, and R. Kaptein. 1979. The aromatic residues of bovine pancreatic ribonuclease studied by ^{1}H nuclear magnetic resonance. *Eur. J. Biochem.* 98:385–397.

Liu, Y. J., D. M. Zhang, and F. J. Rizzo. 1993. Nearly singular and hypersingular integrals in the boundary element method. *In* Boundary Elements XV, Vol. 1. Fluid Flow and Computational Aspects. C. A. Brebbia and J. J. Rencis, editors. Computational Mechanics Publications, Southampton, U.K. 453–468.

Mosher, R. A., D. Dewey, W. Thormann, D. A. Saville, and M. Bier. 1989. Computer simulation and experimental validation of the electrophoretic behavior of proteins. *Anal. Chem.* 61:362–366.

Mosher, R. A., D. A. Saville, and W. Thormann. 1992. The Dynamics of Electrophoresis. VCH, Weinheim, Germany. 236 pp.

Norde, W., and J. Lyklema. 1978. The adsorption of human plasma albumin and bovine pancreas ribonuclease at negatively charged polystyrene surfaces. III. Electrophoresis. *J. Colloid Interface Sci.* 66:277–284.

Nozaki, Y., and C. Tanford. 1967. Examination of titration behavior. *In* Methods in Enzymology, Vol. XI. Enzyme Structure. C. H. W. Hirs, editor. Academic Press, New York. 715–734.

O'Brien, R. W., and L. R. White. 1978. Electrophoretic mobility of a spherical colloidal particle. *J. Chem. Soc. Faraday Trans. 2.* 74:1607–1626.

Rudolphi, T. J., and S. Youn. 1993. Computational alternatives for hypersingular boundary integral equations. *In* Boundary Elements XV, Vol. 1. Fluid Flow and Computational Aspects. C. A. Brebbia and J. J. Rencis, editors. Computational Mechanics Publications, Southampton, U.K. 429–442.

Shugar, D. 1952. The ultraviolet absorption spectrum of ribonuclease. *Biochem. J.* 52:142–149.

Sladek, V., J. Sladek, and M. Tanaka. 1993. Regularization of hypersingular and nearly singular integrals in the potential theory and elasticity. *Int. J. Num. Meth. Eng.* 36:1609–1628.

Solomentsev, Y. E., Y. Pawar, and J. L. Anderson. 1993. Electrophoretic mobility of nonuniformly charged spherical particles with polarization of the double layer. *J. Colloid Interface Sci.* 158:1–9.

Stigter, D. 1978. Electrophoresis of highly charged colloidal cylinders in univalent salt solutions. 2. Random orientation in external field and application to polyelectrolytes. *J. Phys. Chem.* 82:1424–1429.

Swedberg, S. A. 1990. Characterization of protein behavior in high-performance capillary electrophoresis using a novel capillary system. *Anal. Biochem.* 185:51–56.

Tanford, C., and J. D. Hauenstein. 1956. Hydrogen ion equilibria of ribonuclease. *J. Am. Chem. Soc.* 78:5287–5291.

Tanford, C., J. D. Hauenstein, and D. G. Rands. 1955. Phenolic hydroxyl ionization in proteins. II. Ribonuclease. *J. Am. Chem. Soc.* 77: 6409–6413.

Tanokura, M. 1983. ^{1}H nuclear magnetic resonance titration curves and microenvironments of aromatic residues in bovine pancreatic ribonuclease A. *J. Biochem.* 94:51–62.

Teubner, M. 1982. The motion of charged colloidal particles in electric fields. *J. Chem. Phys.* 76:5564–5573.

von Smoluchowski, M. 1921. Elektrische Endosmose und Strömungsströme. *In* Handbuch der Elektrizitat und des Magnetismus. Band II. Stationäre Ströme. L. Graetz, editor. Verlag von Johann Ambrosius Barth, Leipzig, Germany. 366–428.

Yoon, B. J. 1991. Electrophoretic motion of spherical particles with a nonuniform charge distribution. *J. Colloid Interface Sci.* 142:575–581.

Yoon, B. J., and S. Kim. 1989. Electrophoresis of spheroidal particles. *J. Colloid Interface Sci.* 128:275–288.

Yoon, B. J., and A. M. Lenhoff. 1990. A boundary element method for molecular electrostatics with electrolyte effects. *J. Comp. Chem.* 11:1080–1086.

Youngren, G. K., and A. Acrivos. 1975. Stokes flow past a particle of arbitrary shape: a numerical method of solution. *J. Fluid Mech.* 69: 377–403.